

STUDIES OF THE STABILITY AND DYNAMICS OF LEVITATED DROPS

A.V. Anilkumar, C.P. Lee, and T.G. Wang
 Center for Microgravity Research and Applications
 Vanderbilt University
 Nashville, TN 37235, U.S.A.

ABSTRACT

This is a review of our experimental and theoretical studies relating to equilibrium and stability of liquid drops, typically of low viscosity, levitated in air by a sound field^{1,2,3}. The major emphasis here is on the physical principles and understanding behind the stability of levitated drops. A comparison with experimental data is also given, along with some fascinating pictures from high-speed photography. One of the aspects we shall deal with is how a drop can suddenly burst in an intense sound field; a phenomenon which can find applications in atomization technology. Also, we are currently investigating the phenomenon of suppression of coalescence between drops levitated in intense acoustic fields.

INTRODUCTION

In the past two decades, or so, acoustic levitation has gained prominence as a way to manipulate liquid samples in the microgravity environment of Space [4,5,6,7]. This is where the interest in the study of interactions between drops and sound arises. The central question is what happens when a liquid drop is introduced into a standing sound field.

The simplest interaction between the drop and the sound field is the force on the drop. If the drop surface is assumed to be rigid, then the force on the drop [8] is the summation of the normal force acting on the surface due to acoustic radiation pressure $\langle \delta p \rangle$, where [9,10]

$$\langle \delta p \rangle = \frac{\langle p'^2 \rangle}{2\rho_0 c_0^2} - \frac{\rho_0 \langle \mathbf{u} \cdot \mathbf{u} \rangle}{2}, \quad (1)$$

p' is the acoustic pressure, \mathbf{u} is the particle velocity, ρ_0 and c_0 are the density and speed of sound of the ambient air, and $\langle \rangle$ denotes average over an acoustic cycle.

A more complex kind of drop-sound interaction is the deformation of the liquid drop due to the acoustic radiation stress. This is resisted by the drop through its surface tension. The static deformation is described by the Young-Laplace equation

$$P_1 - \langle \delta p \rangle = \sigma \nabla \cdot \mathbf{n}, \quad (2)$$

where σ is surface tension, P_1 is the internal liquid pressure, and $\nabla \cdot \mathbf{n}$ represents the total curvature of the drop surface [11]. Let us consider a drop, of spherical radius R_s , to be at the pressure node of a plane wave $p' = A \sin kz \cos \omega t$, where A is the pressure amplitude, k is the wavenumber, ω is the angular frequency, z is the axial position and t is the time. For small amplitude A , the shape of the drop is given by [12,13]

$$f(\theta) = R_s \left[1 - \frac{3}{32} B_a \left(1 + \frac{7}{5} \alpha^2 \right) P_2(\theta) \right], \quad (3)$$

where $B_a = R_s A^2 / \sigma \rho_0 c_0^2$ is the acoustic Bond number, $\alpha = k R_s < 1$ represents the spherical radius of the drop scaled by the acoustic wavelength $\lambda = 2\pi/k$, and P_2 is a Legendre polynomial. Moderately larger static deformations have been studied numerically by expansion of the drop shape in Legendre polynomials [14]. Also, acoustic deformation can be an excitation source for drop oscillations, if the deforming sound field is modulated in amplitude, near a resonant frequency of the capillary oscillations of the drop [12,15].

EXPERIMENTAL OBSERVATIONS

A common approach to ground-based study of liquid drops is to levitate a millimeter-sized drop in a single-axis acoustic levitator, which consists of a transducer at the bottom and a reflector at the top, providing a standing sound field that vibrates vertically and falls off laterally. It is known that the levitated drop ends up disintegrating in a burst if the sound pressure level (SPL) is raised too high [16]. Our goal is to understand why, when, and how the burst can occur. The first step is to study the phenomenon in detail, using high-speed photography. The observations are described as follows [1,2].

All drops levitated in a sound field become more flattened with increasing SPL, progressively attaining oblate spheroidal, and then flat disk shapes. Their subsequent evolution and stability can be differentiated based on their initial size. Two limiting scenarios can be identified. Whenever the drop is acoustically small ($\alpha \leq 0.3$), flattening cannot exceed a critical point, beyond which the drop disintegrates. The manner of disintegration is a sudden horizontal expansion, in which the drop is pulled apart at the periphery (Fig.1). Acoustically large drops ($\alpha \geq 0.5$), on the other hand, can sustain equilibrium beyond the critical point by actively lowering the sound pressure level in the levitator. A large flattened drop is an efficient scatterer of the acoustic wave and can induce a sufficiently large resonance frequency shift in the system, causing the levitator to lose power [17]. The SPL in the levitator first increases with flattening, as expected, but then decreases with flattening beyond the critical point. Here, the drop becomes concave and eventually drastically flattened to the point where the drop has a meridional cross-section resembling a dogbone, with a membrane in the middle surrounded by a donut-shaped periphery (fig. 2). Drops of intermediate size ($0.3 \leq \alpha \leq 0.5$) lose equilibrium beyond the critical point and show sudden horizontal expansion, but they return to equilibrium following sufficient lowering of the sound pressure level through resonance frequency shift.

On continued flattening, the central membrane of a large drop may eventually buckle upward, with the ring-shaped periphery contracting and closing, leading to violent shattering (Fig.2 f,g,h). The buckling is always upward, such that it has to be related to the presence of gravity. For all low-viscosity drops, like water drops, as the central membrane vibrates in the sound field capillary ripples are excited parametrically on it. Here, unless buckling instability occurs first, the ripples become so intense that satellite droplets are ejected vertically in both directions. This phenomenon is conventionally referred to as atomization. For small drops, on the other hand, atomization takes place near the edge, during the sudden horizontal expansion, and is inherently nonsteady. A highly viscous drop does not atomize, by this route, because any ripple would be heavily suppressed by viscosity.

STATIC EQUILIBRIUM

To understand these complex drop-sound interactions, the natural thing to do is to understand the equilibrium of the system, then find out when the system becomes unstable [1,2,3]. The poles of the drop are stagnation points of the oscillating flow of the sound field. In these regions, according to eq.(1), the radiation stress comes mostly from the acoustic pressure and is positive. At the equator, on the other hand, the particle velocity is most intense. The radiation stress here comes mostly from the particle velocity and is negative. The drop shape is determined by the compressive stress at the poles, the suction stress at the equator, together with surface tension, and the constant internal pressure inside the drop. When the central membrane is thin enough, it vibrates with sound a little. In our cases of interest, the vibration is not strong enough to significantly violate the rigid wall boundary condition. The membrane vibration leads to a Bernoulli correction in the internal pressure. The equilibrium shape, as a consequence of all these forces, changes from an oblate spheroid to one with flat poles, and then to one with concave poles.

Mathematically, the difficulty with the problem of a drastically deformed drop is that the drop shape depends on the wave, but the wave also depends on the shape. To handle the problem in a self-consistent manner, we have used a boundary integral method for solving the Helmholtz equation for the wave [3,18], given the shape. Then we use the resulting radiation pressure to solve for the shape using eq.(2). The two procedures are repeated alternatively until both the wave and the shape converge to their respective forms.

For a given drop size α , if we plot the acoustic Bond number B_a versus the non-dimensional equatorial radius R^* ($R^*=R/R_s$, R : equatorial radius), we find that B_a rises with R^* to a maximum, and then decreases with R^* , schematically as shown by the solid curve in Fig.3. Correspondingly, the SPL increases to a maximum and then decreases with flattening, in agreement with the observation for large drops. A large drop can bring about a downturn in SPL because it can easily induce the necessary resonant frequency shift. Therefore it stays on the solid equilibrium curve until buckling instability, or atomization, occurs. An intermediate sized drop has to expand sufficiently, before it can bring about the necessary lowering in sound intensity, to be on the equilibrium curve. Therefore the drop follows curve 1 (fig. 3) which jumps from the equilibrium curve, but returns to it later. A small drop on the other hand, cannot bring about a significant power loss by resonant frequency shift during expansion. Hence it follows a curve like 2 (fig. 3) to disintegration.

A typical B_a - R^* curve for a large drop is shown in Fig.4, showing good agreement with experiment. When the central membrane of a large drop vibrates, the internal pressure in the membrane cannot be lowered much because the surface curvature of a thin membrane is close to zero. Thereby, the internal pressure has to be close to the external radiation pressure. The Bernoulli effect, due to membrane vibration, is manifested in the relative raising of the liquid pressure in the ring-shaped periphery. This tips the force balance at the edge, such that the drop loses equilibrium at a lower flattening than that for which central membrane does not vibrate. If the drop is viscous, vibration of the membrane is spread into the periphery too, such that Bernoulli effect is effectively nullified and can be ignored. The point here is that a viscous drop can be flattened more than a inviscid drop because of the absence of Bernoulli effect due to membrane vibration. This is consistent with experimental observations.

The actual occurrence of the downturn of the B_a - R^* curve depends on the active involvement of the levitator. In practice, we may be more concerned with drops that are too small to cause any power loss, or a sound system that is too strong to allow for a significant power loss. Hence the peak of a B_a - R^* curve is important because it represents the maximum sound intensity and maximum deformation a drop of size α can sustain. In Fig.5, we plot the maximum B_a , denoted by $B_{a,cr}$, and the corresponding R^* , denoted by R^*_{cr} , versus α . Experimental data are also displayed for comparison, showing good agreement between the two.

INSTABILITIES

On the downturn side of the equilibrium curve (fig. 3), a large drop will lose equilibrium at the edge, beyond a certain degree of flattening. But before the drop reaches this point, instabilities will occur. These can be either: (i) the buckling instability [1] or, (ii) the parametric instability that gives rise to the ripples and the subsequent atomization [2, 19].

Buckling instability is explained as follows. When a drop is drastically flattened such that the membrane is thin enough to be forced into vibration, like a drumhead by the sound field, a dynamic pressure arises. The latter is given by $\rho \langle v^2 \rangle / 2$, where ρ is the density of the liquid, and v is the vibration velocity of the membrane. This pressure tends to push the liquid toward the periphery. If equilibrium is to be maintained, the hydrostatic pressure in the membrane has to become lower, as dictated by Bernoulli law. But the membrane surfaces are almost flat, such that there is limited room for readjustment. The membrane becomes more susceptible to acoustic vibration as it gets thinner with flattening. Ultimately, there is a point beyond which the hydrostatic pressure in the membrane can no longer withhold the dynamic pressure. If the membrane is perfectly symmetric about its mid-surface, there is still the relatively higher hydrostatic pressure in the thick periphery to contain the membrane liquid. But in the presence of gravity, the membrane is slightly buckled upward, to start with. In this case, the dynamic pressure can cause the membrane to expand and buckle upward, as shown in Fig.2 (f,g,h).

For a low viscosity drop, capillary ripples can be excited on the membrane through parametric instability, when the membrane vibrates in the sound field (frequency ω). In general, there can be two wave modes: a symmetric wave (frequency ω_s) in which the two surfaces vibrate in opposite directions, and an antisymmetric wave (frequency ω_a) in which they vibrate in the same direction [20]. For a vibrating membrane, of a given thickness, the wavelength of the disturbance is determined as a consequence of parametric instability [2,19]. Parametric excitation of a wavelength can occur only when the wavelength satisfies the synchronism condition: $\omega = \omega_s + \omega_a$. When the membrane is thick

$\omega_a = \omega_s = \omega/2$, and the waves are known as Faraday ripples. When the ripples grow violent, they spit out satellite droplets as in conventional atomization. When the membrane is thin, ω_a is much larger than ω_s . A thin film will shatter as ripples grow because it will snap wherever its two surfaces come into contact. If a drop is very viscous, then ripples are suppressed. The easier route for a viscous drop to fragment is through a sudden horizontal expansion, in which the membrane is stretched so thin that it has to rupture and shatter due to van der Waals forces.

CLOSING COMMENTS

In this article, we have addressed the issue of equilibrium and stability of a liquid drop, when introduced into an intense sound field. This complex problem has been primarily presented in a physical way, substantiating it with clear photographic evidence and a simple theoretical framework employing the acoustic Bond number and the drop equatorial radius (B_a - R^* curve). Presently, we are trying to understand the mechanism of suppression of coalescence of drops in intense acoustic fields. Normally, when two drops are introduced into a levitating field, they coalesce to form a single drop. However, whenever the intensity of the acoustic field is high, the two drops do not coalesce, but instead form a stable doublet (fig. 6 a,b). They seem to contact along a line, and their contacting surfaces display a knife-edge feature. The reason for this stability has probably to do with the nature of the vibrating air flow in the narrow strait between the drops, and needs to be well understood²¹. The stable doublet can be rotated as a rigid body, without the two drops separating. The drops coalesce only when the intensity of the levitating field is reduced, thereby making the drops less flattened and more spherical.

ACKNOWLEDGEMENTS

The work described in this article was carried out at the Center for Microgravity Research and Applications at Vanderbilt University, under funding by the Microgravity Science and Applications Division of the National Aeronautics and Space Administration. Figures 1 - 4 have been reproduced with permission of the Physics of Fluids journal, a publication of the American Institute of Physics.

REFERENCES

1. Lee, C.P., Anilkumar, A.V., & Wang, T.G. 1991, Phys. Fluids A3, 2497.
2. Anilkumar, A.V., Lee, C.P., & Wang, T.G. 1993, Phys. Fluids A5, 2763.
3. Lee, C.P., Anilkumar, A.V., & Wang, T.G. 1994, Phys. Fluids 6, 3554.
4. Wang, T.G. 1979, In: IEEE, Ultrasonic Symposium Proceedings, page 471.
5. Wang, T.G., Anilkumar, A.V., Lee, C.P., & Lin, K.C. 1994, J. Fluid Mech. 276, 389.
6. Wang, T.G., Anilkumar, A.V., Lee, C.P., & Lin, K.C. 1994, J. Colloid Interface Sci. 165, 19.
7. Wang, T.G., Anilkumar, A.V., & Lee, C.P. 1996, J. Fluid Mech. 308, 1.
8. King, L.V. 1934, Proc. R. Soc. Lond. A147, 212.
9. Beyer, R.T. 1974, Nonlinear Acoustics, Naval Ship Systems Command, Department of the Navy.
10. Lee, C.P. & Wang, T.G. 1993, J. Acoust. Soc. Am. 94, 1099.
11. Lamb, H. 1945, Hydrodynamics, Dover, sixth edition.
12. Marston, P.L. 1980, J. Acoust. Soc. Am. 67, 15.
13. Trinh, E.H. & Hsu, C.J. 1986, J. Acoust. Soc. Am. 79, 1335.
14. Tian, Y., Holt, R.G., & Apfel, R.E. 1993, J. Acoust. Soc. Am. 93, 3096.
15. Marston, P.L. & Apfel, R.E. 1980, J. Acoust. Soc. Am. 67, 27.
16. Lierke, E.G., Leung, E.W., & Luhmann, D. 1988, In: Wang, T.G. (editor), AIP Conference Proceedings 197, Drops and Bubbles Third International Colloquium, Monterey, California, pg. 71.
17. Leung, E., Lee, C.P., Jacobi, N., & Wang, T.G. 1982, J. Acoust. Soc. Am. 72, 615.
18. Batchelor, G.K. 1967, An introduction to Fluid Dynamics, Cambridge.
19. Danilov, S.D. & Mironov, M.A. 1992, J. Acoust. Soc. Am. 92, 2747.
20. Taylor, G.I. 1959, Proc. R. Soc. Lond. A253, 296.
21. Dell'Aversana, P., Banavar, J.R., and Koplik, J. 1996 Phys. Fluids 8, 15.

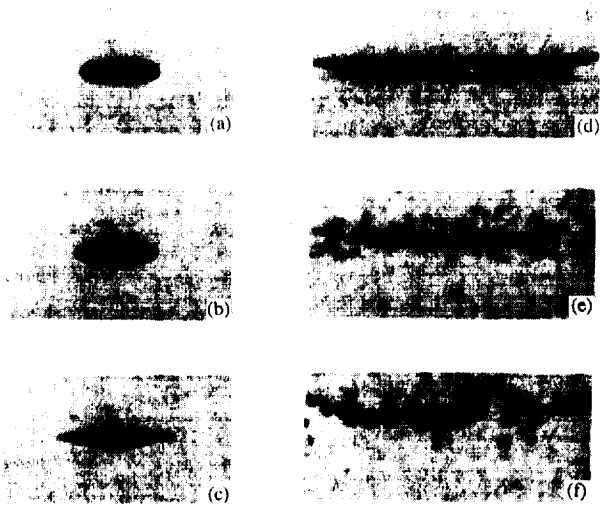


Fig. 1 The side view of a small water drop ($\alpha=0.2$): (a) being flattened, (b) its rim getting sharper, (c) rim developing into a knife-edge, (d,e) expanding horizontally and instability occurring along the outermost edge, and (f) final breakup.

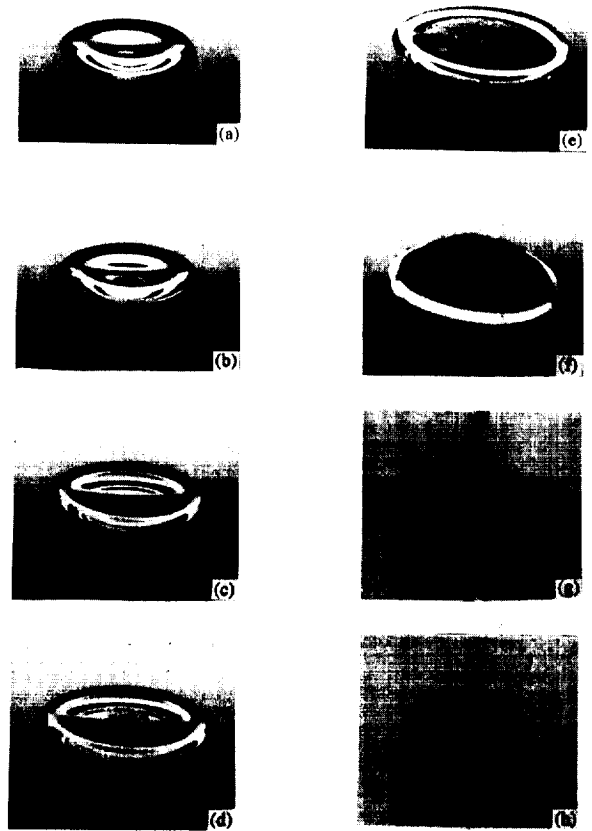


Fig. 2. The evolution of a large water drop ($\alpha=0.8$) levitated in an acoustic field with increasing intensity: (a) being flattened and slightly dimpled, (b,c) becoming concave, (d,e) ripples formed on the central membrane, spreading throughout the latter, (f) buckling upward, (g) ballooning with two jets shooting in opposite directions at the bottom part that has just been closed, and (h) final breakup.

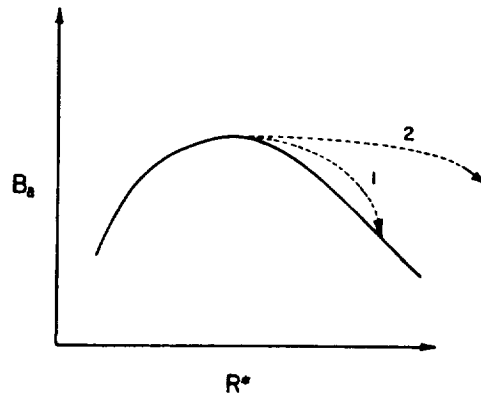


Fig. 3. Responses of a levitated drop to a continuous increase in input sound intensity.

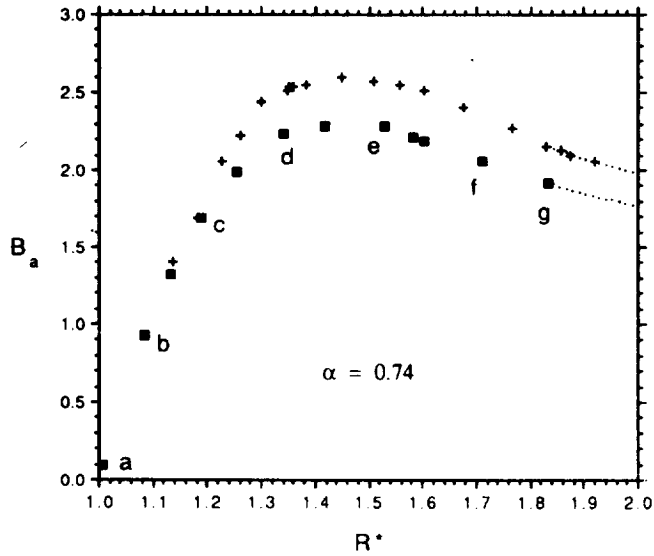


Fig. 4. Plot of B_a vs R^* for a water drop with $\alpha=0.74$. The crosses are experimental data and the solid squares are theoretical data. The dotted curves are asymptotic forms given by $B_a=B_m^*/R^*$, where $B_m^*=3.52$ for the theory and 3.95 for the experiment.

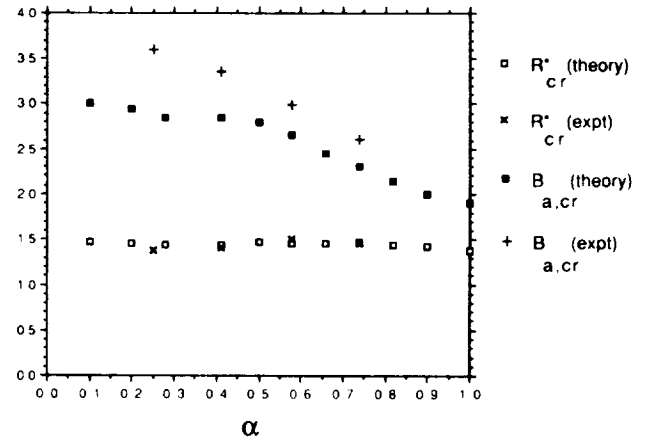


Fig. 5. The maximum B_a of the B_a - R^* curve, denoted by $B_{a,cr}$, and the corresponding R^* , denoted by R_{cr}^* , for a range of α . Theoretical data are given by squares and experimental data are given by crosses.



Fig. 6. Side (a) and top (b) views of a stable non-coalescing doublet in intense acoustic field.